

CALCULATION OF TURBULENT GAS-DISPERSION FLOWS IN CHANNELS WITH RECIRCULATION EDDIES

L. I. Zaichik, M. V. Kozelev, and V. A. Pershukov

UDC 532.529.5:532.517.4

Gas-dispersion turbulent flows in a plane channel with expansion behind a step and in a cylindrical chamber with sudden expansion are numerically simulated on the basis of the Euler two-velocity description.

Applications of the so-called Euler approach are considered. This is based on the use of equations of the same mathematical type for describing the motion of both carrier and dispersed phases in recirculating turbulent gas-dispersion flow calculations. In dispersed flow calculations the application of the Euler approach has been most successful, as a rule, in the case of relatively simple flows such as jets and flows in straight channels [1-10], when the flow is almost unidirectional and the solution of the system of equations in the boundary layer approximation applies.

Examples of the use of the Euler approach for describing complicated gas-dispersion flows of pronounced two- or three-dimensional character are very limited [11-14]. In this paper, in order to establish the advantage (or at least competitiveness) of the Euler approach over the widely used mixed Euler-Lagrange method for describing turbulent dispersion flows numerical results are presented for two-dimensional flows in a plane channel with step expansion and in a cylindrical combustion chamber with sudden expansion. The calculations are based on the models developed in [4,8,10,15].

1. For constructing the system of equations governing the motion of a dispersed phase of low volume concentration the equation for the probability density function (PDF) of the particle velocity in turbulent flow is used [15]:

$$\frac{\partial P}{\partial \tau} + v_k \frac{\partial P}{\partial x_k} + \frac{\partial}{\partial v_k} \left(\frac{U_k - v_k}{\tau_u} + F_k \right) P = \frac{f_u}{\tau_u} \langle u_i' u_k' \rangle \frac{\partial^2 P}{\partial v_i \partial v_k} + g_u \langle u_i' u_k' \rangle \left(\frac{\partial^2 P}{\partial x_i \partial v_k} + \frac{\partial V_n}{\partial x_k} \frac{\partial P}{\partial v_i \partial v_n} \right) \quad (1.1)$$

where τ is time, U_k and u_k are the averaged and pulsating components of the gas velocity, V_k is the dispersed phase velocity, F_k is the gravity acceleration, τ_u is the dynamic relaxation time, and $\langle u_i' u_k' \rangle$ are the second single-point single-time moments of the pulsating gas velocity.

The coefficients of involvement of the particles in the pulsating motion of the carrier phase, f_u and g_u , are chiefly determined by the structure of the energy-containing turbulent vortices and, in the case of a piecewise-constant approximation of the two-time correlation function of the pulsating gas velocity along the particle trajectories, have the form [4]:

$$f_u = 1 - \exp\left(-\frac{T_p}{\tau_u}\right), \quad g_u = \frac{T_p}{\tau_u} - 1 + \exp\left(-\frac{T_p}{\tau_u}\right) \quad (1.2)$$

where T_p is the characteristic time of interaction between the particles and energy-containing vortex gas formations (turbulent moles).

Integrating (1.1) over the entire velocity space and decomposing the averaged velocity of the dispersed phase into a sum of convection and diffusion terms [8,10] gives the equations of diffusion and motion of the particles:

$$\frac{\partial \Phi}{\partial \tau} + \frac{\partial \Phi V_k}{\partial x_k} = \frac{\partial}{\partial x_i} \left(D_{ik}^p \frac{\partial \Phi}{\partial x_k} \right) \quad (1.3)$$

$$\frac{\partial \Phi V_i}{\partial \tau} + \frac{\partial \Phi V_i V_k}{\partial x_k} = -\frac{\partial \Phi \langle v_i' v_k' \rangle}{\partial x_k} + \Phi \left(\frac{U_i - V_i}{\tau_u} + F_i \right) \quad (1.4)$$

$$D_{ik}^p = \tau_u g_u \langle u_i' u_k' \rangle = \tau_u g_u D_{ik} / T_u, \quad D_{ik} = T_u \langle u_i' u_k' \rangle$$

where Φ is the averaged volume concentration of the dispersed phase, V_i is the convection component of the dispersed phase velocity (with the same notation as the total averaged velocity), D_{ik}^p is the particle diffusion tensor, D_{ik} is the tensor of turbulent diffusion of the inertialess admixture, T_u is the Lagrangian time macroscale of turbulence, and $\langle v_i' v_k' \rangle$ are the turbulent stresses in the dispersed phase.

The equations for Φ and V_i , (1.3) and (1.4), obtained from the equation for the PDF (1.1), are the same as the corresponding equations in [8,10] obtained from averaging the equations of mass and momentum conservation with the volume concentration used as a weighting function. The equations for the second moments of the velocity pulsations obtained by these two methods are also identical [8,10,15]. From these equations, taking into account the isotropy of the convection and diffusion terms and also the generation tensor in the equation for the second moments, the following algebraic expressions for the turbulent stresses in the dispersed phase can be obtained [8,10,15]:

$$\langle v_i' v_k' \rangle = \frac{2}{3} k_p \delta_{ik} - \nu_p \left(\frac{\partial V_i}{\partial x_k} + \frac{\partial V_k}{\partial x_i} - \frac{2}{3} \frac{\partial V_n}{\partial x_n} \delta_{ik} \right) \quad (1.5)$$

$$\nu_p = f_u \nu_t + \frac{1}{3} \tau_u k_p, \quad k_p = \frac{1}{2} \langle v_k' v_k' \rangle$$

Here, ν_p is the particle turbulent viscosity coefficient, ν_t is the gas turbulent viscosity coefficient, and k_p is the particle turbulent energy.

The equation for the particle turbulent energy takes the form

$$\frac{\partial \Phi k_p}{\partial \tau} + \frac{\partial \Phi V_k k_p}{\partial x_k} = -\frac{\partial}{\partial x_k} \left(\Phi \frac{\langle v_k' v_n' v_n' \rangle}{2} \right) - \Phi \langle v_i' v_k' \rangle \frac{\partial V_i}{\partial x_k} + \frac{2\Phi}{\tau_u} (f_u k - k_p) \quad (1.6)$$

where k is the turbulent energy of the gas.

The diffusion term in (1.6) is determined with the use of the equations for the third moments of the velocity pulsations, which follow from (1.1). A certain simplification leads to the expression [15]

$$\frac{\langle v_k' v_n' v_n' \rangle}{2} = -\Lambda_p \frac{\partial k_p}{\partial x_k}, \quad \Lambda_p = \frac{10}{27} \tau_u (k_p + g_u k) \quad (1.7)$$

The expression for the diffusion term obtained in [10] is analogous to (1.7) with the only difference that there is no second term in parentheses in the expression for the turbulent energy diffusion coefficient Λ_p . However, this difference is not essential because for inertial particles ($\tau_u / T_p > 1$) the coefficient g_u is small, whereas for small particles ($\tau_u / T_p < 1$) the whole diffusion term makes practically no contribution to the turbulent energy balance in the dispersed phase.

The averaged motion of the gas phase is governed by the continuity and momentum balance equations

$$\partial U_k / \partial x_k = 0 \quad (1.8)$$

$$\frac{\partial U_i}{\partial \tau} + U_k \frac{\partial U_i}{\partial x_k} = -\frac{1}{\rho} \frac{\partial P}{\partial x_i} + \nu \frac{\partial^2 U_i}{\partial x_k \partial x_k} - \frac{\partial \langle u_i' u_k' \rangle}{\partial x_k} - \frac{\rho_p \Phi}{\rho \tau_u} (U_i - V_i) + F_i \quad (1.9)$$

where ρ , ρ_p are the densities of the gas and particle material, and P is the pressure.

The turbulent stresses in the gas phase were determined according to the gradient representation

$$\langle u_i' u_k' \rangle = \frac{2}{3} k \delta_{ik} - \nu_t \left(\frac{\partial U_i}{\partial x_k} + \frac{\partial U_k}{\partial x_i} \right) \quad (1.10)$$

The turbulent properties of the gas were calculated on the basis of the two-parameter k - ϵ model of turbulence.

Taking into account the reverse influence of the particles, the equations for the gas turbulent energy k and its dissipation ε are written in the form:

$$\frac{\partial k}{\partial \tau} + U_k \frac{\partial k}{\partial x_k} = \frac{\partial}{\partial x_k} \left(\frac{v_i}{\sigma_k} \frac{\partial k}{\partial x_k} \right) - \langle u_i' u_k' \rangle \frac{\partial U_i}{\partial x_k} - \quad (1.11)$$

$$\varepsilon - \frac{\rho_p}{\rho \tau_u} \left[2\Phi(1 - f_u)k - \tau_u g_u \langle u_i' u_k' \rangle (U_i - V_i) \frac{\partial \Phi}{\partial x_k} \right]$$

$$\frac{\partial \varepsilon}{\partial \tau} + U_k \frac{\partial \varepsilon}{\partial x_k} = \frac{\partial}{\partial x_k} \left(\frac{v_i}{\sigma_\varepsilon} \frac{\partial \varepsilon}{\partial x_k} \right) - C_{\varepsilon 1} \frac{\varepsilon}{k} \langle u_i' u_k' \rangle \frac{\partial U_i}{\partial x_k} -$$

$$C_{\varepsilon 2} \frac{\varepsilon^2}{k} - \frac{2\rho_p \varepsilon}{\rho \tau_u} \left[\Phi(1 - f_\varepsilon) - \frac{\tau_u g_\varepsilon}{3} (U_k - V_k) \frac{\partial \Phi}{\partial x_k} \right] \quad (1.12)$$

$$f_\varepsilon = 1 - \exp\left(-\frac{T_\varepsilon}{\tau_u}\right), \quad g_\varepsilon = \frac{T_\varepsilon}{\tau_u} - 1 + \exp\left(-\frac{T_\varepsilon}{\tau_u}\right).$$

The turbulent viscosity coefficient of the gas is determined by the relationship

$$v_t = \frac{C_\mu}{1 + (P_k/\varepsilon - 1 - A_k/\varepsilon)C_1} \frac{k^2}{\varepsilon}$$

$$P_k = \frac{P_{nn}}{2}, \quad P_{ij} = -\left(\langle u_i' u_k' \rangle \frac{\partial U_j}{\partial x_k} + \langle u_j' u_k' \rangle \frac{\partial U_i}{\partial x_k} \right), \quad A_k = \frac{A_{nn}}{2}, \quad (1.13)$$

$$A_{ij} = \frac{\rho_p}{\rho \tau_u} \left\{ 2\Phi(1 - f_u) \langle u_i' u_j' \rangle - g_u [\langle u_i' u_k' \rangle (U_j - V_j) + \langle u_j' u_k' \rangle (U_i - V_i)] \frac{\partial \Phi}{\partial x_k} \right\}.$$

Here, P_{ij} and A_{ij} determine respectively the generation of turbulent stresses in the gas phase due to the averaged motion and the reverse influence of the particles on the turbulent stresses in the gas. Expression (1.13) was obtained on the basis of a Rodi transformation of the equations for the second moments of the gas velocity pulsations with the aim of reducing them to algebraic form [16] using the isotropic representation for the tensors P_{ij} and A_{ij}

$$P_{ij} = -\frac{2}{3} k \left(\frac{\partial U_i}{\partial x_j} + \frac{\partial U_j}{\partial x_i} \right), \quad A_{ij} = \frac{2}{3} A_k \delta_{ij}.$$

For $P_{ij} = \varepsilon$ and $A_k = 0$ (1.13) turns into the expression for the turbulent viscosity coefficient commonly used in the standard two-parameter model of turbulence. In (1.13) a correction function accounts for the influence of the turbulence nonequilibrium and the dispersed phase on v_t . It should be noted that both expression (1.13) and the experimental dependence for a single-phase shear layer obtained by Rodi [16] predict the same type of influence of the turbulence nonequilibrium on v_t : as P_k/ε increases the turbulent viscosity coefficient decreases.

The values of the constants in (1.11) and (1.12) are standard for the two-parameter model of turbulence [17]: $\sigma_k = 1.0$, $\sigma_\varepsilon = 1.3$, $S_{\varepsilon 1} = 1.44$, $C_{\varepsilon 2} = 1.92$, $C_\mu = 0.09$. The constant C_1 in (1.13) corresponds to the constant in the Rotta approximation for the exchange terms in the equations of balance of the second moments of the velocity pulsations. For C_1 the mean of the commonly used values is assumed: $C_1 = 2.0$ [16].

The isotropic expression $D_{ik} = D_i \delta_{ik}$, where $D_i = \nu / Sc_i$ and the turbulent Schmidt number $Sc_i = 0.8$, is assumed for D_{ik} , the coefficient of turbulent diffusion of the inertialess admixture in terms of which the particle diffusion coefficient, D_{ik}^p in (1.3), is expressed.

The characteristic time of interaction of the particles and the energy-containing vortex formations of the gas is determined by the expression

$$T_p = T_u / \sqrt{1 + (T_u |U - V|/L)^2} \quad (1.14)$$

where $L = (2k/3)^{1/2} T_u$ is the length macroscale of turbulence.

The time macro- and microscales of turbulence are determined by the expressions

$$T_* = \alpha \frac{k}{\varepsilon}, \quad \alpha = \frac{3C_p}{2Sc_t}, \quad T_* = \sqrt{\frac{15\nu}{\varepsilon}} \quad (1.15)$$

Now, with (1.2), (1.5), (1.7), (1.10), and (1.13)-(1.15) taken into account, the system of equations (1.3), (1.4), (1.6), (1.8), (1.9), (1.11), (1.12) gives a closed description of the turbulent gas dispersion flow.

2. To solve equations (1.3), (1.4), (1.6) governing the motion of the dispersed phase the boundary conditions must be prescribed on the surfaces bounding the flow. As in case of deriving boundary conditions in the theory of a rarefied gas [18], for constructing boundary conditions for the equations of the dispersed phase motion the particle PDF in the near-wall region must be known. The boundary conditions were derived in [4,7] from the solution of the equation for PDF obtained by the perturbation method and in [6,9] with the use of a PDF prescribed *a priori* as a δ -function or as a quasinormal velocity distribution.

We will give the boundary conditions for particles which are not absorbed by the wall and assume elastic interaction between particles and wall in the normal direction, that is allowing only for the possible loss of tangential momentum. In this case the probability density for the particle transition from state 1 before interaction (collision) with a wall to state 2 after interaction is given by the expression

$$P_w(v_2/v_1) = \delta(v_{x2} - \Phi v_{x1}) \delta(v_{y2} + v_{y1})$$

where x and y are the coordinates normal and tangential to the wall, and Φ is the momentum recovery coefficient for the collision with the wall.

For zero dispersed-phase mass flux through the wall according to (1.3)

$$y=0: \quad V_y = \frac{\partial \Phi}{\partial y} = 0 \quad (2.1)$$

Taking into account (1.5), in the case under consideration the expression for the tangential stress at the wall [7,9]

$$\langle v_x' v_y' \rangle = -\frac{1 - \Phi}{1 + \Phi} \sqrt{\frac{2 \langle v_y'^2 \rangle}{\pi}} V_x$$

gives the boundary condition for the tangential velocity of the dispersed phase

$$y=0: \quad v_p \frac{\partial V_x}{\partial y} = \frac{1 - \Phi}{1 + \Phi} \sqrt{\frac{4k_p}{3\pi}} V_x \quad (2.2)$$

Expression (2.2) is a boundary condition of the third kind. From (2.2) it follows that due to the dynamic inertia of the particles there may be a velocity slip on the surface. For an ideally smooth wall the recovery coefficient $\Phi = 1$, while for a very rough wall we may assume $\Phi = 5/7$ [19,20].

In agreement with the assumption of elastic interaction between the particles and the wall in the normal direction $\partial \langle v_y'^2 \rangle / \partial y = 0$ at $y=0$. Hence the boundary condition for (1.6) can be written in the form:

$$y=0: \quad \partial k_p / \partial y = 0 \quad (2.3)$$

According to (2.3) the turbulent energy of the dispersed phase may be nonzero on the wall in spite of the zero value of the turbulent energy of the carrier flow. The presence of dispersed phase velocity fluctuations near the wall is due to the transfer of pulsation from the turbulent region of the flow because of particle inertia.

As boundary conditions for the equations of averaged motion of the gas phase (1.8), (1.9) no-slip conditions are prescribed on the walls:

$$y=0: \quad U_i = 0 \quad (2.4)$$

For determining the pulsation properties of the flow near the wall it is worth using the method of wall functions which has gained wide acceptance in monophase flow calculation [17]. Introducing wall functions considerably reduces the number of computational grid points in the direction normal to the wall. In this case the boundary conditions for the equations (1.11), (1.12) are prescribed not on the wall itself but at some distance from it, outside the viscous sublayer in the so-called logarithmic layer. The basis of the wall function method involves the assumption of constant turbulent shear stress $\langle u_x' u_y' \rangle$ and turbulent energy k and also of universality of the profile of the velocity component U_x parallel to the surface in the near-wall region, where the first calculation grid point for the equations (1.11), (1.12) is

positioned.

The analysis of the system of equations for the second moments of the gas-phase velocity pulsations shows that the gas turbulent energy in the logarithmic layer in the presence of a dispersed phase can be determined with fair accuracy from the relationship

$$k = u_*^2 C_\mu^{-1/2} \quad (2.5)$$

where u_* is the dynamic velocity.

In the logarithmic layer the dissipation rate is determined by the expression

$$\varepsilon = C_\mu^{3/4} k^{3/2} / \kappa y \quad (2.6)$$

where for monophasic flow the Prandtl-Karman constant $\kappa = 0.4$. Assuming that the length scale of turbulence is not much affected by the agents complicating the flow, κ may be taken to be equal to the Prandtl-Karman constant in a two-phase flow also.

The dynamic velocity u_* and the gas friction on the wall $\tau_w = \rho u_*^2$ can be found from the universal logarithmic velocity profile in the near-wall region

$$u_* = \frac{U_x}{u_*} = \frac{\ln y_*}{\kappa} + A, \quad y_* = \frac{y u_*}{\kappa} \quad (2.7)$$

The applicability of the wall law (2.7) with the same values of the constants κ and A as in monophasic flow was experimentally confirmed for vertical and horizontal gas-dispersion flows in [21].

Therefore, expressions (2.1)-(2.7) determine the boundary conditions on rigid surfaces for the system of equations of the motion of a turbulent gas dispersion flow.

As the inlet boundary conditions we used the distributions of U_x , k , and ε , which were uniform over the channel cross-section, while in the channel outlet the solution was assumed to be continuous up to the second derivatives with respect to the longitudinal coordinate.

3. On the basis of the system of equations described above the aerodynamics of a combustion chamber were calculated. The combustion chamber is a cylindrical channel with a sudden expansion into which a gas-dispersion mixture is injected through two inlet nozzles, separating the mixture into primary and secondary flows (Fig. 1). The dispersed phase is injected into the near-axis region of the chamber and mixes with pure air. Due to the sudden expansion there is a recirculation region.

The streamlines in Fig. 1a clearly demonstrate that the velocity fields in different chamber cross-sections are substantially nonuniform. As the distance from the axis increases, the stream function levels on each of the streamlines are 0.1, 0.25, 0.5, 0.75, 1.0, 1.1, 1.2 and characterize the mass flux through the outlet cross-section normalized with the inlet flow rate. Figures 1b-d show the velocity profiles for the gas flow (b), particles 46 μm in diameter (c), and particles 100 μm in diameters. The broken line joins together the points of zero particle velocity in each cross-section.

The results of a comparisons with the experimental data [22] (Fig. 1b) confirm that the averaged gas velocity is satisfactorily described within the framework of the model used. The velocity profiles for particles of different size and the gas velocity profile differ considerably from each other. For large particles the profile of V_x is flatter and in the limit $\tau_\mu \rightarrow \infty$ the dispersed-phase motion is analogous to the translational movement of a rigid body. This correlates well with the experimental data for flows in tubes [23].

In agreement with the tendency for the large particle velocity vector to remain parallel to the initial one, there is a decrease in the degree of involvement of the dispersed phase in the circulating motion. With increase in the particle size the region of negative velocities shrinks sharply, so that the carrier and dispersed phase velocities are not only quite different in value but even act in opposite directions. Therefore the residence times for particles of different sizes may differ several-fold.

In accordance with the gradient representation of the turbulent stress tensor in the gas (1.10) and dispersed (1.5) phases, the substantial nonuniformity of the averaged gas and particle velocities results in sharp variation of the turbulence pulsation field over the cross-section. The maximum level of the turbulence pulsations (about 10-15% of the maximum averaged velocity) is located in the region separating the main and reversed flows.

Because of this nonuniform distribution of the turbulent energy with a deep minimum in the near-axis flow region there is a potential barrier for the particles. This is due to the turbulent migration (a turbophoresis force) directed toward decreasing pulsation energy of the gas [4]. The turbophoresis force drastically reduces the diffusion exchange of particles between the regions of direct and recirculating flow. This decreases the probability of particle penetration

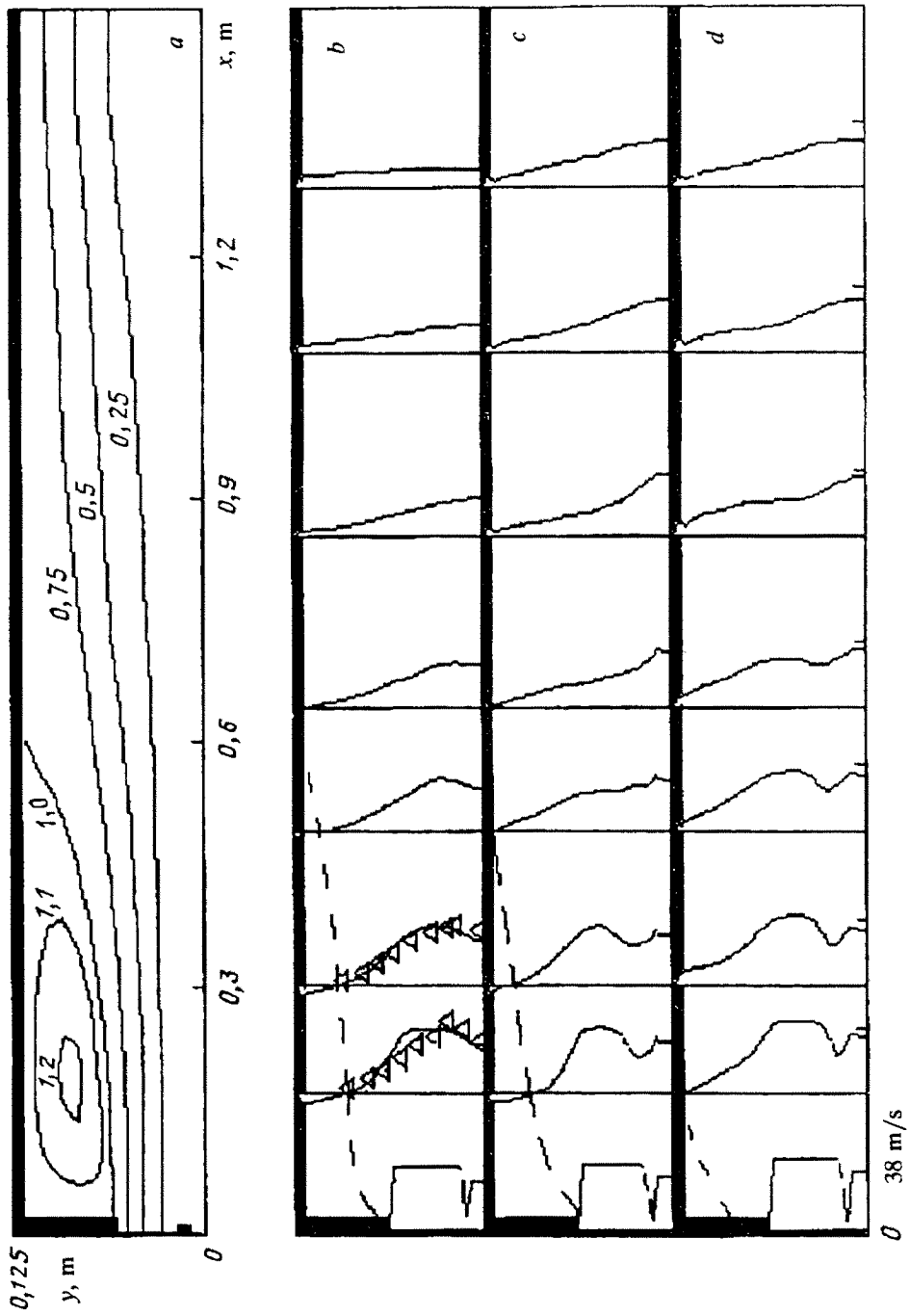


Fig. 1

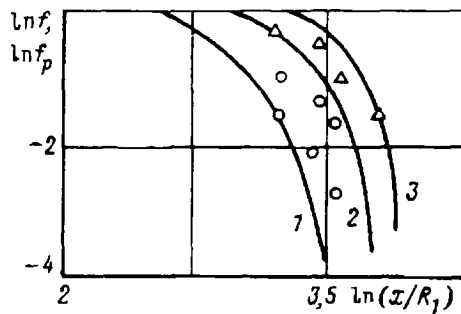


Fig. 2

into the reversed flow region and inhibits the mixing processes.

Figure 2 shows the variation along the device axis of the dispersed-phase mixing function $f_p = \Phi V_x / \Phi_0 V_{x0}$ and the passive scalar $f = m_i / (m_1 + m_2)$ (where m_i is the mass flux of the scalar admixture in the primary ($i=1$) and the secondary ($i=2$) flows). Curve 1 corresponds to the mixing of a passive scalar, 2 is for a dispersed phase with particle diameter $19 \mu\text{m}$, 3 is for a dispersed phase with particle diameter $54 \mu\text{m}$ (experimental data from [22]), and R_1 is the radius of the central injection nozzle for the gas-dispersed flow. The inertial admixture mixes much more slowly than an inertialess one. An increase in particle size further reduces the mixing (curve 3).

For more a detailed analysis of the dynamics of particles of various diameters in recirculating eddies calculations were performed for a gas-dispersion flow in a plane channel with a backward-facing step. The geometry of the channel with a step corresponds to the experimental unit described in [24] and is shown in Fig. 3a. The Reynolds number formed from the step height H was assumed to be $Re = U_0 H / \nu = 3 \cdot 10^5$, where U_0 is the gas inlet velocity. The streamlines characterizing the flow pattern are shown in Fig. 3a. On each isolate the values of the stream function correspond to the notation in Fig. 1a. The velocity profiles for gas, particles with $d_p = 30 \mu\text{m}$, and particles with $d_p = 70 \mu\text{m}$ are shown in Fig. 3b-d respectively.

With increase in particle diameter the degree of particle involvement into the recirculating motion decreases. Large particles completely retain the initial direction of the motion. This manifests itself in the absence of negative velocities throughout the flow. On the whole, the general flow pattern is quite similar to that considered above for the flow in a combustion chamber.

For the flows under consideration the importance of the correct formulation of the boundary conditions for the pulsating energy of the dispersed phase should be mentioned. The phenomenon of nonzero pulsating energy on the channel walls, described above, is of fundamental importance. The use of the locally uniform approximation for the particle turbulent energy in the form $k_p = f_i k$ results in the nonphysical growth of the dispersed phase concentration near the wall. The concentration growth is due to the conservation of the particle pulsation energy flux $\Phi k_p = \text{const}$ near the wall from which it follows that $\Phi \rightarrow \infty$ for $k_p \rightarrow 0$. The use of the differential equation (1.6) for k_p and the boundary condition (2.3) ensures quite satisfactory physical results.

For a quantitative comparison of the calculational results with the experimental data [24] we analyzed the variation of the maximum positive velocity V_{max}^+ along the channel and the maximum negative velocity V_{max}^- along the recirculation eddy. These relations are shown in Figs. 4 and 5, where $V^{\pm} = V_{\text{max}}^{\pm} / U_0$, $x' = (x_r - x) / x_r$, and x_r is the coordinate of the reattachment point of the recirculation eddy. Curve 1 corresponds to the gas flow, curve 2 is for the particle velocity with $d_p = 15 \mu\text{m}$, and curve 3 is for the particle velocity with $d_p = 30 \mu\text{m}$. In both the calculations and the experiments with increase in the particle diameter the maximum of the negative velocity of the dispersed phase moves toward the step (upstream).

Therefore, the calculational results confirm the correctness of the description of the averaged characteristics of complicated gas dispersion turbulent flows with recirculation regions within the framework of the proposed model. For the calculation of the dispersed phase characteristics in bounded flows it is necessary to use the equation for the particle pulsation energy, because the use of the locally uniform approximation results in considerable errors in the near-wall region of the flow.

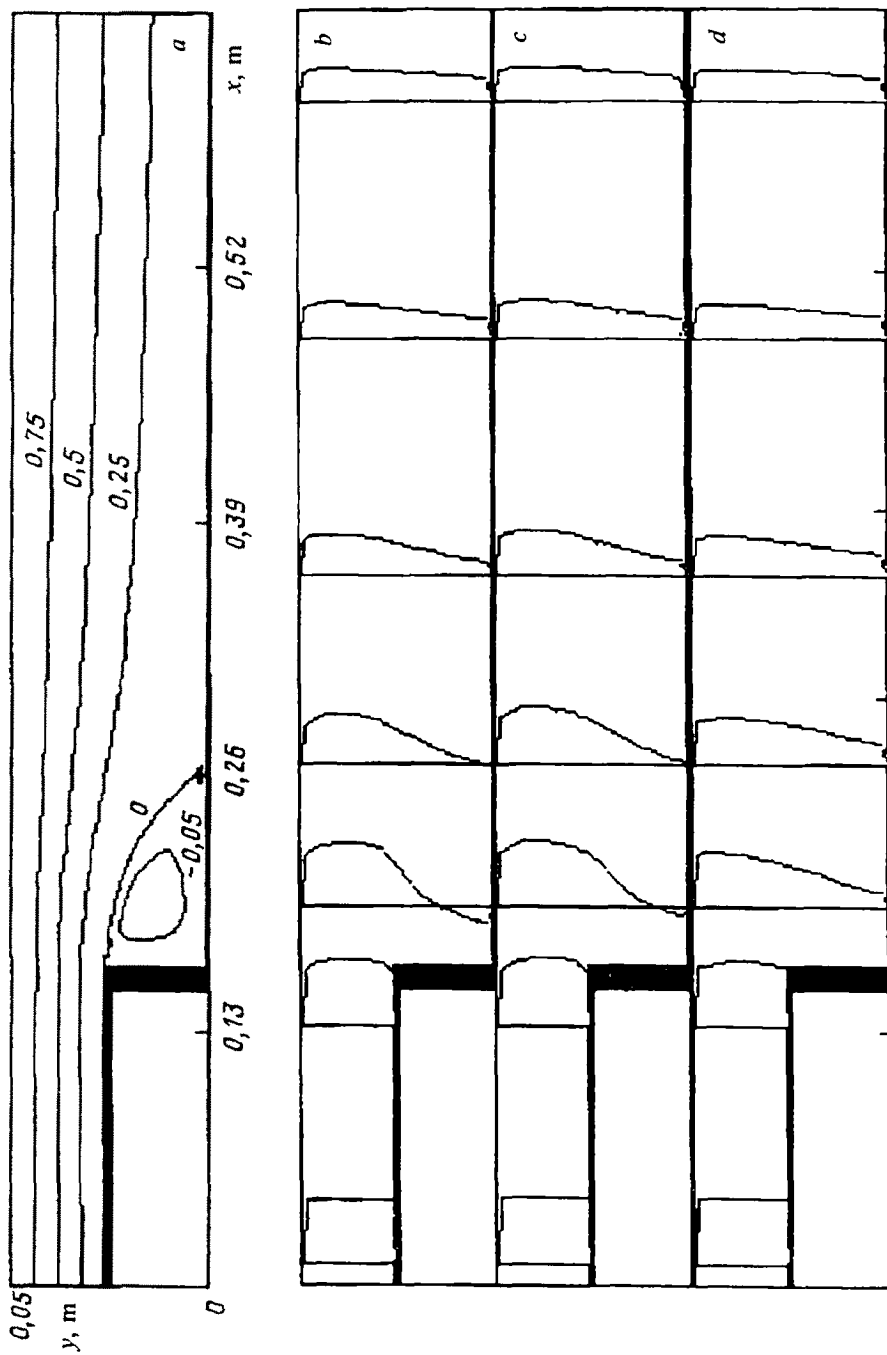


Fig. 3

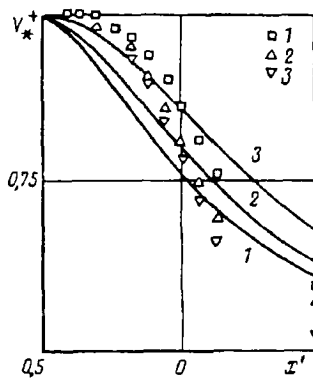


Fig. 4

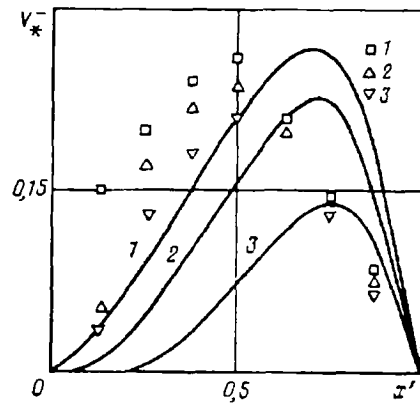


Fig. 5

The work was financially supported by the Russian Foundation for Fundamental Research (project code 93-02-15902).

REFERENCES

1. C. P. Chen and P. E. Wood, "Turbulence closure modeling of the dilute gas-particle axisymmetric jet," *AIChE Journal*, **32**, No. 1, 163-166 (1986).
2. A. A. Shraiber, L. B. Gavin, V. A. Naumov, and V. P. Yatsenko, *Turbulent Gas-Dispersion Flows*, [in Russian], Naukova Dumka, Kiev (1987).
3. A. A. Mostafa and H. C. Mongia, "On the modeling of turbulent evaporating sprays: Eulerian versus Lagrangian approach," *Int. J. Heat and Mass Transfer*, **30**, No. 12, 2583-2593 (1987).
4. I. V. Derevich and L. I. Zaichik, "Particle deposition from a turbulent flow," *Fluid Dynamics*, **23**, No. 5, 722-729 (1988).
5. M. A. Rizk and S. E. Elghobashi, "A two-equation turbulence model for dispersed dilute confined two-phase flows," *Int. J. Multiphase Flow*, **15**, No. 1, 119-133 (1989).
6. L. V. Kondrat'ev and V. V. Shor, "Investigation of gas-particle turbulent pipe flow with allowance for collisions with the wall and particle rotation," *Fluid Dynamics*, **25**, No. 1, 46-53 (1990).
7. I. V. Derevich and V. M. Eroshenko, "Calculation of the average phase velocity slip in turbulent multiphase channel flow," *Fluid Dynamics*, **25**, No. 2, 221-229 (1990).
8. A. A. Vinberg, L. I. Zaichik, and V. A. Pershukov, "Model for calculating of turbulent gas-dispersion jet flows," *Inzhenerno-Fizicheskii Zhurnal*, **61**, No. 4, 554-563 (1991).
9. I. N. Gusev, E. I. Guseva, and L. I. Zaichik, "Model of particle deposition from turbulent gas-solid flow in channels with absorbent walls," *Fluid Dynamics*, **27**, 43-48 (1992).
10. A. A. Vinberg, L. I. Zaichik, and V. A. Pershukov, "Calculation of the momentum and heat transfer in turbulent gas-particle jet flows," *Fluid Dynamics*, **27**, No. 3, 353-362 (1992).
11. F. Pourahmadi and J. A. C. Humphrey, "Modeling solid-fluid turbulent flows with application to predicting erosive wear," *Phys. Chem. Hydrodyn.*, **4**, No. 3, 191-219 (1983).
12. B. Dobrowolski, "A computational model for the prediction of two-dimensional non-equilibrium turbulent recirculating two-phase flow," *Arch. Mech.*, **38**, No. 5-6, 611-634 (1986).
13. T. Hong and L. Zhou, "Numerical simulation of three-dimensional turbulent gas-particle flows in boiler furnaces by a continuum model of particle phase," in: *Proc. 1-st Asian-Pacific Int. Symp. on Combustion and Energy Utilization. Beijing, 1990*, Beijing, 184-189 (1990).
14. O. Simonin, "Second-moment prediction of dispersed phase turbulence in particle-laden flows," in: *Proc. 8th Symp. on Turbulent Shear Flows. Munich, 1991*, Munich, pp.7.4.1-7.4.6 (1991).
15. L. I. Zaichik, "Models of turbulent momentum and heat transfer in dispersed phase based on the equations for second and third moments of pulsation of particle velocity and temperature," *Inzhenerno-Fizicheskii Zhurnal*, **63**, No. 4, 404-413 (1992).
16. W. Rodi, "Turbulent models for environment," in: *Prediction Methods for Turbulent Flows*, Hemisphere Publ. Corp. (1980).
17. B. E. Launder and D. B. Spalding, "The numerical computation of turbulent flow," *Comput. Math. Appl. Mech. Eng.*, **2**, 269-289 (1974).
18. M. N. Kogan, *Dynamics of a Rarefied Gas* [in Russian], Nauka, Moscow (1967).
19. M. A. Gol'dshtik and A. K. Leont'ev, "On the collision of a sphere and a rigid surface," *Inzhenerno-Fizicheskii Zhurnal*, **3**, No. 11, 83-88 (1960).
20. V. A. Naumov, "Two approaches to the description of the collision of a spherical body and a rough wall," *Prikl. Mekhanika*, **25**, No. 5, 116-119 (1989).
21. N. I. Gel'perin, V. G. Ainshtein, L. I. Krupnik, and Z. N. Mamedlyayev, "Hydrodynamic resistance of gas-dispersion flows," *Izv. Vusov, Energetika*, No. 1, 94-99 (1976).
22. Y. B. Hahn and H. Y. Sohn, "The trajectories and distribution of particles in a turbulent axisymmetric gas jet injected into a flash furnace shaft," *Met. Trans. B*, **19B**, No. 1, 871-884 (1988).
23. L. S. Lee and F. Durst, "On the motion of particles in turbulent duct flows," *Int. J. Multiphase Flow*, **8**, No. 1, 124-146 (1982).
24. B. Ruck and B. Makiola, "Particle dispersion in a single-sided backward-facing step flow," *Int. J. Multiphase Flow*, **14**, No. 6, 787-800 (1988).